Long wave interaction with a moored elastic plate floating near an inclined beach

Yifeng Yang[a, b], Kang Ren[a], Luofeng Huang[b], Michael H. Meylan[c]
[a] Department of Mechanical Engineering, University College London, London, UK.
[b] School of Water, Energy and Environment, Cranfield University, Cranfield, UK.
[c] School of Information and Physical Sciences, University of Newcastle, Callaghan, Australia.
Email: yifeng.yang.19@ucl.ac.uk

Highlights

- An analytical scheme is developed for wave-elastic plate interaction near an inclined beach.
- The linearized shallow water equation is employed for calculation efficiency.
- Analysis is provided for the wave runup on the beach and strain on the plate.

1. Introduction

Solar photovoltaics are widely acknowledged as pivotal technology for mitigating global carbon emissions [1]. In contrast to other energy power plants, solar photovoltaic power generation is proportional to its surface coverage, necessitating a considerably large area to deploy an industrial-scale power plant. One popular scenario is to develop floating photovoltaics (FPV) on oceans [2], especially near the coastlines, which allows solar farms to benefit from the existed power transmission and distribution networks, leading to cost savings. In this paper, the interaction between long waves and a solar farm floating near an inclined beach is investigated analytically. The floating solar coverage is modelled as an elastic thin plate. Unlike related studies that focus on finite water depth [3], in our work, we consider the physical scenario in a shallow water region, and the fluid is described by the linearized shallow water equation. This approach not only conforms to the physics reality but is also more efficient in addressing the sloping region and in terms of calculation.

2. Mathematical modelling and solution procedure

The problem of interaction between waves and an elastic plate floating near an inclined beach is sketched in Figure 1. A Cartesian coordinate system O-xz is established with the origin at the intersection point of the sloping beach and the mean water surface. The x-axis is reversely along the mean water surface, and the z-axis points upwards. The slope angle of the beach is denoted by β. The mean water depth, $h(x)$, is constant, equalling to h_0, at the flat seabed region, and $h(x) = -x\tan\beta$ at the sloping beach region. An incident wave comes from $x = -\infty$ and will be scattered by the elastic plate covering the water surface at $x_1 \le x \le x_2$, where $x_2 = x_1 + d$ with $x_2 \le x_3 = -h_0\cot\beta$, and d represents the length of the plate. It is assumed that two edges of the plate at $x = x_{1,2}$ are each connected to the seabed by mooring lines.

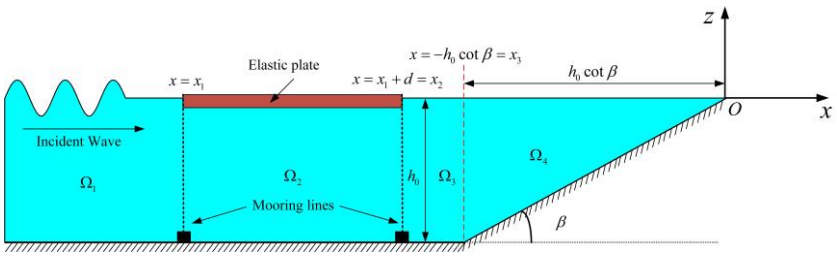

Figure 1: Illustration of the problem.

The incoming wave is assumed to be periodic in time t with radial frequency ω. Hence, the velocity potential and wave elevation can be written as $\Phi(x,t) = \mathrm{Re}\{\phi(x)e^{\mathrm{i}\omega t}\}$ and $W(x,t) = \mathrm{Re}\{\eta(x)e^{\mathrm{i}\omega t}\}$. A domain decomposition approach is used to treat this problem. As shown in Figure 1, the entire domain are divided into four subdomains, namely Ω_1 ($-\infty < x < x_1$), Ω_2 ($x_1 \le x \le x_2$), Ω_3 ($x_2 < x \le x_3$) and Ω_4 ($x_3 < x \le 0$). We may use $\phi^{(j)}$ to represent the spatial velocity potential in Ω_j ($j = 1\sim4$). Under the linearized shallow water wave assumption [4], the velocity potential is assumed to be a constant along the z-direction, which is only valid when the wavelength $\lambda \gg h_0$. $\phi^{(j)}$ ($j = 1, 3$) are governed by

$$\frac{\mathrm{d}^2\phi^{(i)}(x)}{\mathrm{d}x^2} + \frac{\omega^2}{gh_0}\phi^{(i)}(x) = 0, \qquad x \in \Omega_i \ (i = 1, 3), \tag{1}$$

where g represents the acceleration due to gravity. $\phi^{(2)}$ satisfies

$$\left[L\frac{\mathrm{d}^6}{\mathrm{d}x^6} + (\rho g - m_e\omega^2)\frac{\mathrm{d}^2}{\mathrm{d}x^2} + \frac{\rho\omega^2}{h_0}\right]\phi^{(2)}(x) = 0, \qquad x \in \Omega_2, \tag{2}$$

where $L = Eh_e^3/[12(1-\nu^2)]$ is the flexural rigidity and $m_e = \rho_e h_e$ is the mass per unit area of the plate, with E, ν, ρ_e and h_e denoting the Young's modulus, Poisson's ratio, density and thickness of the plate, respectively. ρ represents the density of water. From Synolakis [5], $\phi^{(4)}$ is governed by

$$\left[\frac{x\tan\beta}{h_0}\frac{\mathrm{d}^2}{\mathrm{d}x^2} + \frac{\tan\beta}{h_0}\frac{\mathrm{d}}{\mathrm{d}x} - \frac{\omega^2}{gh_0}\right]\phi^{(4)}(x) = 0, \qquad x \in \Omega_4. \tag{3}$$

At the interfaces $x = x_j$ ($j = 1, 2, 3$), the continuity of pressure and horizontal velocity requires

$$\phi^{(j)}(x_j) = \phi^{(j+1)}(x_j), \qquad \frac{\mathrm{d}\phi^{(j)}(x_j)}{\mathrm{d}x} = \frac{\mathrm{d}\phi^{(j+1)}(x_j)}{\mathrm{d}x}, \qquad j = 1, 2, 3. \tag{4a, b}$$

The spatial wave elevation $\eta(x)$ can be expressed as

$$\eta(x) = \begin{cases} \mathrm{i}\frac{h_0}{\omega}\frac{\mathrm{d}^2\phi}{\mathrm{d}x^2} & x_1 \le x \le x_2 \\ -\frac{\mathrm{i}\omega}{g}\phi & \text{others} \end{cases}. \tag{5}$$

At the edges of the plate, mooring lines are used to connect the elastic plate to the seabed to maintain its stability. In such a case, the bending moment and shear force of the plate satisfy

$$\begin{cases} \frac{\mathrm{d}^2\eta(x_j)}{\mathrm{d}x^2} = 0 \\ L\frac{\mathrm{d}^3\eta(x_j)}{\mathrm{d}x^3} = q_j\eta(x_j) \end{cases}, \qquad j = 1, 2, \tag{6a, b}$$

where q_j denotes the stiffness of the mooring lines at x_j.

To solve the boundary value problem, we may employ the method of matched eigenfunction expansion. As a result, $\phi^{(1)}(x)$ and $\phi^{(3)}(x)$ can be written as

$$\phi^{(1)}(x) = Ie^{-\mathrm{i}\hbar_0 x} + Re^{\mathrm{i}\hbar_0 x}, \qquad x \in \Omega_1, \tag{7}$$

$$\phi^{(3)}(x) = Ce^{-\mathrm{i}\hbar_0 x} + De^{\mathrm{i}\hbar_0 x}, \qquad x \in \Omega_3, \tag{8}$$

where $\hbar_0 = \omega/\sqrt{gh_0}$ denotes the wave number, $I = \mathrm{i}Ag/\omega$ with A denotes the amplitude of the incoming wave. R, C and D are unknown coefficients. Similarly, $\phi^{(2)}(x)$ provides

$$\phi^{(2)}(x) = \sum_{m=-2}^{0}\left(A_m e^{-\mathrm{i}\kappa_m x} + B_m e^{\mathrm{i}\kappa_m x}\right), \qquad x \in \Omega_2. \tag{9}$$

where A_m and B_m are unknwon coefficients, κ_m ($m = -2, -1, 0$) satisfy

$$L\kappa_m^6 + (\rho g - m_e\omega^2)\kappa_m^2 - \frac{\rho\omega^2}{h_0} = 0, \tag{10}$$

where κ_{-2} and κ_{-1} are two complex roots with negative imaginary part, and $\kappa_{-2} = -\bar{\kappa}_{-1}$. κ_0 is the positive real root. $\phi^{(4)}$, governed by the nonlinear Eq. (3), can be solved analytically by using variable substitution. Letting $\xi = 2\hbar_0\sqrt{-xh_0\cot\beta}$, we obtain

$$\frac{\mathrm{d}^2\phi^{(4)}(x)}{\mathrm{d}x^2} + \frac{1}{\xi}\frac{\mathrm{d}\phi^{(4)}(x)}{\mathrm{d}x} + \phi^{(4)}(x) = 0. \tag{11}$$

Eq. (11) is the zero-th order Bessel equation, which gives

$$\phi^{(4)}(x) = F\mathcal{J}_0(\xi) = F\mathcal{J}_0\left(2\hbar_0\sqrt{-xh_0\cot\beta}\right), \tag{12}$$

where $\mathcal{J}_n$ denotes the n-th Bessel function of the first kind, and F is an unknown coefficient. To solve the above 10 unknown coefficients, we may match the velocity potential at $x = x_j$ ($j = 1, 2, 3$) by using Eq. (4), which yields the following six linear equations

$$\begin{cases} Re^{\mathrm{i}\hbar_0 x_1} - \sum_{m=-2}^{0}\left(A_m e^{-\mathrm{i}\kappa_m x_1} + B_m e^{\mathrm{i}\kappa_m x_1}\right) = -Ie^{-\mathrm{i}\hbar_0 x_1} \\ \mathrm{i}\hbar_0 Re^{\mathrm{i}\hbar_0 x_1} - \mathrm{i}\sum_{m=-2}^{0}\left(-\kappa_m A_m e^{-\mathrm{i}\kappa_m x_1} + \kappa_m B_m e^{\mathrm{i}\kappa_m x_1}\right) = \mathrm{i}\hbar_0 Ie^{-\mathrm{i}\hbar_0 x_1} \\ Ce^{-\mathrm{i}\hbar_0 x_2} + De^{\mathrm{i}\hbar_0 x_2} - \sum_{m=-2}^{0}\left(A_m e^{-\mathrm{i}\kappa_m x_2} + B_m e^{\mathrm{i}\kappa_m x_2}\right) = 0 \\ -\mathrm{i}\hbar_0 Ce^{-\mathrm{i}\hbar_0 x_2} + \mathrm{i}\hbar_0 De^{\mathrm{i}\hbar_0 x_2} - \mathrm{i}\sum_{m=-2}^{0}\left(-\kappa_m A_m e^{-\mathrm{i}\kappa_m x_2} + \kappa_m B_m e^{\mathrm{i}\kappa_m x_2}\right) = 0 \\ Ce^{\mathrm{i}\hbar_0 h_0\cot\beta} + De^{-\mathrm{i}\hbar_0 h_0\cot\beta} = F\mathcal{J}_0(2\hbar_0 h_0\cot\beta) \\ -\mathrm{i}\hbar_0 Ce^{\mathrm{i}\hbar_0 h_0\cot\beta} + \mathrm{i}\hbar_0 De^{-\mathrm{i}\hbar_0 h_0\cot\beta} = F\hbar_0\mathcal{J}_1(2\hbar_0 h_0\cot\beta) \end{cases}. \tag{13a~f}$$

Four extra equations can be also obtained from the edge conditions in Eq. (6), or

$$\begin{cases} \sum_{m=-2}^{0}\kappa_m^4\left(A_m e^{-\mathrm{i}\kappa_m x_j} + B_m e^{\mathrm{i}\kappa_m x_j}\right) = 0 \\ \sum_{m=-2}^{0}\left[\left(-\mathrm{i}L\kappa_m^5 + q_j\kappa_m^2\right)A_m e^{-\mathrm{i}\kappa_m x_j} + \left(\mathrm{i}L\kappa_m^5 + q_j\kappa_m^2\right)B_m e^{\mathrm{i}\kappa_m x_j}\right] = 0 \end{cases}, \; j = 1, 2. \tag{14a, b}$$

Using Eqs. (13) and (14), all the unknown coefficients listed above can be solved.

3. Results and analysis

In the following calculations, the typical values of the elastic plate and the fluid are chosen as

$$\rho = 1025\ \mathrm{kgm^{-3}},\ \ h_0 = 20\mathrm{m},\ \ g = 9.81\ \mathrm{ms^{-2}}, \rho_e = 0.9\rho,\ \ E = 5\ \mathrm{GPa},\ \ \nu = 0.3. \tag{15}$$

All the variables and numerical results are presented in the non-dimensionalized form based on a combination of ρ, g and h_0.

The wave runup at $x = 0$, or $|\eta(0)|/A$, versus wave period T under different values of plate thickness h_e and plate length d are displayed in Figure 2(a) and (b), respectively. We observe that $|\eta(0)|/A$ shows an oscillatory behaviour with T when there exists a floating elastic plate, or $h_e > 0$. Besides, such oscillation phenomenon becomes much more obvious as h_e and d increase. From the aspect of coastal engineering, the presence of the elastic plate sometimes cannot work as a wave barrier to reduce the wave runup at the shore, and even cause more significant wave elevation on the shore. Moreover, Figure 3 also illustrated that long waves are less affected by the elastic plate. The maximum principal strain in the elastic plate can be calculated by

$$\epsilon_{max} = \max\left\{\left|\frac{h_e}{2}\frac{\mathrm{d}^2\eta(x)}{\mathrm{d}x^2}\right|\right\} = \max\left\{\left|\frac{\mathrm{i}h_0 h_e}{2\omega}\sum_{m=-2}^{0}\kappa_m^4\left(A_m e^{-\mathrm{i}\kappa_m x} + B_m e^{\mathrm{i}\kappa_m x}\right)\right|\right\}. \tag{16}$$

ϵ_{max} versus the slope angle β and the stiffness q_1 and q_2 are presented in Figure 3, where a similar oscillatory behaviour of ϵ_{max} versus T is observed. In Figure 3(a), this oscillatory behaviour becomes weaker as the increase of β, and less peaks can be observed in the curves of ϵ_{max} versus T. Figure 3(b) demonstrates that the strain induced by long waves may be increased if larger stiffnesses are used.

4. Conclusions

The interaction between waves and a moored elastic plate floating near an inclined beach is investigated analytically. Typical results and discussions are made on the wave runup on the beach, and the maximum principal strain on the elastic plate. It is found that they both show oscillatory behaviour with the wave period, and this phenomenon is affected by typical physical parameters of the plate and the beach, such as the slope angle of the beach, thickness & length of the elastic plate, as well as stiffness of the mooring lines.

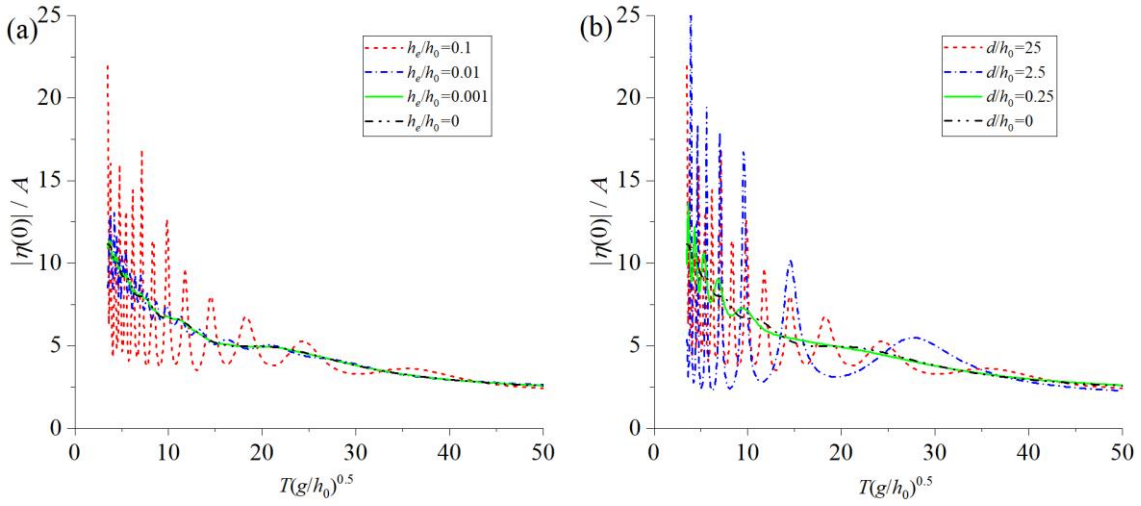

Figure 2. Wave runup at $x = 0$. (a) $d/h_0 = 25$ and varying h_e/h_0. (b) $h_e/h_0 = 0.1$ and varying d/h_0. ($\beta = 10^o$, $q_1/\rho g h_0 = q_2/\rho g h_0 = 4.973 \times 10^{-1}$, $(x_3 - x_2)/h_0 = 0.5$)

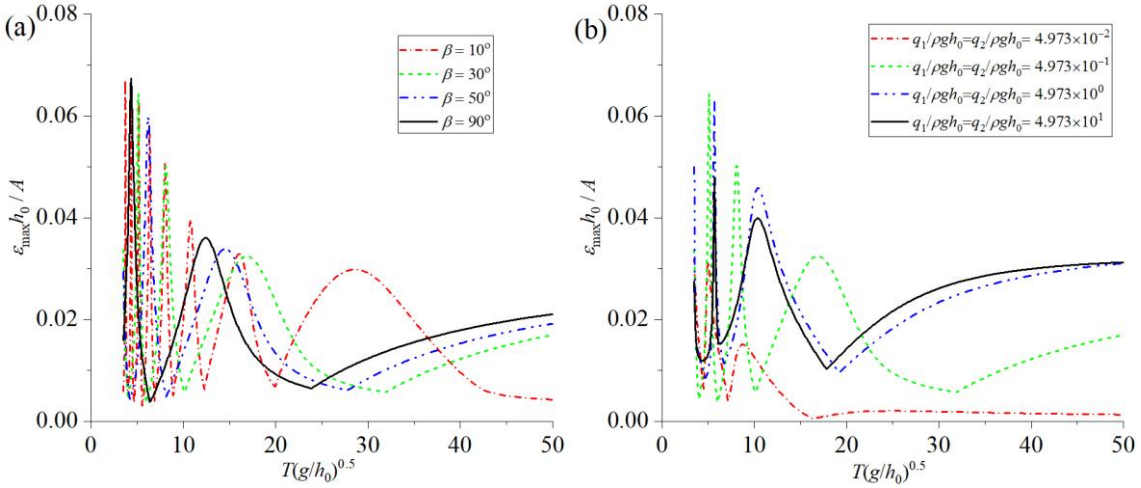

Figure 3. Maximum principal strain in the elastic plate. (a) Under different β, $q_1/\rho g h_0 = q_2/\rho g h_0 = 4.973 \times 10^{-1}$. (b) Under different q_1 & q_2, $\beta = 30^o$. ($h_e/h_0 = 0.1$, $d/h_0 = 5$, $(x_3 - x_2)/h_0 = 0.5$)

Acknowledgement

KR acknowledges funding support from the Royal Society (IEC\NSFC\223358) and Lloyds Register Foundation (N21\100005). LFH acknowledges grants from Innovate UK (No. 10048187, 10079774, 10081314) and the Royal Society (IEC\ NSFC\ 223253, RG\R2\232462).

References

[1] Almeida, R. M., Schmitt, R., Grodsky, S. M., Flecker, A. S., Gomes, C. P., Zhao, L., Liu, H. H., Barros, N., Kelman, R. & McIntyre, P. B. (2022). Floating solar power could help fight climate change—let's get it right. Nature, 606, 246-249.

[2] Sahu, A., Yadav, N. & Sudhakar, K. (2016). Floating photovoltaic power plant: A review. Renewable and sustainable energy reviews, 66, 815-824.

[3] Ren, K., Wu, G. X., & Thomas, G. A. (2016). Wave excited motion of a body floating on water confined between two semi-infinite ice sheets. Physics of Fluids, 28(12).

[4] Ohkusu, M. & Namba, Y. (2004). Hydroelastic analysis of a large floating structure. Journal of Fluids and Structures, 19, 543-555.

[5] Synolakis, S. E. (1987). The runup of solitary waves, J. Fluid Mech., 185, 523-545.